Current and current fluctuations in quantum shuttles

Antti–Pekka Jauho,[1,*] Christian Flindt,[1,†] Tomáš Novotný,[1,2,‡] and Andrea Donarini[1,§]

[1]*MIC - Department of Micro and Nanotechnology,*
Technical University of Denmark, DTU - Building 345east,
DK-2800 Kongens Lyngby, Denmark

[2]*Department of Electronic Structures,*
Faculty of Mathematics and Physics, Charles University,
Ke Karlovu 5, 121 16 Prague, Czech Republic

(Dated: February 2, 2008)

Abstract

We review the properties of electron shuttles, i.e. nanoelectromechanical devices that transport electrons one-by-one by utilizing a combination of electronic and mechanical degrees of freedom. We focus on the extreme quantum limit, where the mechanical motion is quantized. We introduce the main theoretical tools needed for the analysis, e.g. generalized master equations and Wigner functions, and we outline the methods how the resulting large numerical problems can be handled. Illustrative results are given for current, noise, and full counting statistics for a number of model systems. Throughout the review we focus on the physics behind the various approximations, and some simple examples are given to illustrate the theoretical concepts. We also comment on the experimental situation.

PACS numbers: 85.85.+j, 72.70.+m, 73.23.Hk, 73.63.-b

I. INTRODUCTION

As advances in technology push the size of the electronic components towards the nanometer scale, the well-established technology of Micorelectromechanical Systems (MEMS) begins to acquire quantum features. This trend signals the birth of a new research field, Nanoelectromechanical Systems (NEMS). Despite of the infancy of NEMS, a large literature is already available on it, and for a broad overview the interested reader is referred to recent review articles[1,2,3]. The review at hand has a more restricted scope: it is devoted to a theoretical analysis of a very specific NEMS device, the electron shuttle. By presenting a detailed study of such an idealized model system we hope to be able to illustrate the basic physics and conceptual problems that need to be understood before a general theory of NEMS can be developed.

The electron shuttle, originally introduced by Gorelik *et al.* in 1998[4], consists of a movable nanoscopic grain which is coupled via tunnel barriers to source and drain electrodes. A subtle combination of quantum transport and the mechanical degrees of freedom play an essential role for the functionality of the device. The device can exhibit a "phase transition": when a control parameter is tuned (this could be the damping of the oscillator), at a certain threshold value the system enters a new transport regime, the shuttle regime, where charge is transported in an orderly fashion (i.e. essentially a fixed number charges per mechanical oscillation cycle). (This phenomenon is particularly pronounced if the device operates in the strong Coulomb blockade regime, when only one excess charge at a time is allowed in the movable part.) In the original suggestion of Ref. 4 the motion of the movable grain was treated macroscopically, i.e., with Newton's equation of motion. In our group we have been asking questions of what happens when the movable body is so light that also its motion becomes quantized. For example, does the shuttle transition persist in the quantum regime? Another interesting question concerns the interpretation of measurements of NEMS devices, possibly exhibiting shuttling. As it turns out, a measurement of the stationary IV-characteristics does not always yield enough information to uniquely identify the underlying microscopic charge transport mechanism. A point in case is the C_{60} SET experiment by Park et al.[5] where two alternative interpretations, namely incoherent phonon assisted tunneling[6,7,8,9] or shuttling,[4,10] are plausible. The *current noise* provides another important characteristics, supplementary to the mean current.[11,12,13] The Fano factor

which characterizes the degree of correlation between charge transport events is a powerful diagnostic tool to distinguish between various transport mechanisms. Therefore, studies of the current noise in NEMS have become an active field of research.[14,15,16,17,18,19,20] Based on studies where the mechanical system is treated classically, one expects a giant enhancement of noise at the shuttling transition[18], and we want to investigate whether this also occurs in the quantum case. One can go even further along this line: why stop at the current noise, which is the second cumulant of the *full counting statics* (FCS)? Surely FCS (which equals the probability $P_n(t)$ of n electrons being collected, say, in the right lead at time t) will contain even more detailed information. Consequently, FCS in mesoscopic devices has been a very active research field for some time now, and its importance and relevance have been underlined by a recent *measurement* of the third cumulant[21]. Thus, FCS for NEMS is obviously an interesting issue. We are aware of a recent calculation for a classical, driven shuttle[15], and at the end of this paper we illustrate some of our own very recent generalizations of these concepts to the quantum regime using a simple example; a full description will be given elsewhere[22].

We have investigated quantum shuttles in several recent papers,[19,22,23,24,25,26] where the full technical details can be found; the purpose of the present paper is to introduce some of the basic issues to a more general reader. Several other groups have also recently studied quantum shuttles, see e.g. Refs. 27,28,29,30. The paper is organized as follows. In Section 2 we introduce the models of quantum shuttles employed in our work. The total Hamiltonian consisting of the "system" (both mechanical and electronic degrees of freedom of the quantum dot array), the leads, and a generic heat bath is used to illustrate the derivation of a Markovian generalized master equation (GME) which is the starting point of the theoretical analysis. Along the way from the Hamiltonian to the generalized master equation we identify the necessary assumptions, and point out several issues of potential importance not addressed so far within the field of NEMS.

In Section 3 we discuss the calculation of the current and the zero-frequency component of the current noise spectrum for a NEMS device described by a GME. We also give a qualitative discussion of the required numerical calculations, which are highly non-trivial due to the large dimensions of the involved matrices. Finally, some examples of our numerical results are displayed. Section 4 is devoted to an elementary discussion of the calculation of the full counting statistics, and a brief review of the experimental status.

II. THE MODEL

At least two model systems have been considered in the literature. Gorelik *et al.*[4] considered a single movable quantum dot, while Armour and MacKinnon[31] introduced a model of a three-dot array whose central dot is movable, see Fig.1. Both of these systems are of intrinsic interest and may find applications in real systems. The quantum system is assumed to be in the strong Coulomb blockade regime in which only none or one extra (spinless) electron in the whole system are allowed. Thus, in the one-dot case the electronic states are $|0\rangle$ and $|1\rangle$, while in the triple-dot case we have $|0\rangle, |L\rangle, |C\rangle$, and $|R\rangle$. The quantum system is coupled to two leads with a high bias applied between them. The bias is smaller than the charging energy for addition or removal of other electrons but otherwise it is the largest energy scale in the model.

The moving dot interacts with its surroundings and its dissipative dynamics is described by the interaction with a generic heat bath. The Hamiltonian has the form

$$\hat{H} = \hat{H}_{\rm osc} + \hat{H}_{\rm el} + \hat{H}_{\rm el-leads}(\hat{x}) + \hat{H}_{\rm leads} + \hat{H}_{\rm bath} + \hat{H}_{\rm osc-bath} \tag{1}$$

where

$$\hat{H}_{\rm osc} = \frac{\hat{p}^2}{2m} + \frac{m\omega_0^2\hat{x}^2}{2} \tag{1a}$$

describes the mechanical center-of-mass motion of the central dot as a one-dimensional harmonic oscillator with mass m and frequency ω_0. We emphasize the importance of the nonlinear dependence of $\hat{H}_{\rm el-leads}$ on the oscillator degree of freedom; the $\hat{x}$-dependence is often exponential which lies at the heart of the shuttling instability. We refer to the literature for explicit expressions for the other terms appearing in Eq.(1)[4,23,31]. The leads are held at different electrochemical potentials $\mu_{L,R}$ whose difference gives the bias across the array (see Fig. (1)). We assume that the tunneling densities of states are independent of energy. This is necessary for the *first Markov approximation*,[32] used later on, to hold. Further, as already implied above, we assume $\mu_L \to \infty$, $\mu_R \to -\infty$. These assumptions are necessary for the derivation of the Markovian dynamics of the movable system. Finally, the heat bath consisting of an infinite set of harmonic oscillators linearly coupled to the mechanical degree of freedom is described with the Caldeira-Leggett model[33] in its Ohmic form.

A. Generalized Master Equation

For the description of the model we use the language of quantum dissipative systems.[33] As the "system" (or "device") we take the electronic states plus the one-dimensional oscillator describing the center-of-mass motion of the central dot. The electronic leads and the heat bath interacting with the mechanical degree of freedom constitute the reservoirs. The task is to integrate out the degrees of freedom of the reservoirs to end up with an equation of motion for the system density operator. The derivation proceeds in two steps first integrating out the leads and then the heat bath in the weak coupling limit to get the desired GME for the system density operator. We remark that the assumed additivity of the two heat baths should be proven, however we are not aware of any such proof.

As a specific example of an end result of this procedure, we give the GME governing the system density operator in the one-dot case, written here in a Liouvillean form:

$$\dot{\rho}(t) = \mathcal{L}\rho(t) = (\mathcal{L}_{\rm coh} + \mathcal{L}_{\rm driv} + \mathcal{L}_{\rm damp})\rho(t) \tag{2}$$

where the various *superoperators* $\mathcal{L}_i$, i= coh, driv, damp, are defined as

$$\mathcal{L}_{\rm coh}\rho = \frac{1}{i\hbar}[H_{\rm osc} + \varepsilon_0 c_0^\dagger c_0 - eExc_0^\dagger c_0, \rho] \ , \tag{3}$$

$$\begin{aligned}\mathcal{L}_{\rm driv}\rho = &-\frac{\Gamma_L}{2}\big(c_0 c_0^\dagger e^{-\frac{2x}{\lambda}}\rho - 2c_0^\dagger e^{-\frac{x}{\lambda}}\rho e^{-\frac{x}{\lambda}}c_0 + \rho e^{-\frac{2x}{\lambda}}c_0 c_0^\dagger\big) \\ &- \frac{\Gamma_R}{2}\big(c_0^\dagger c_0 e^{\frac{2x}{\lambda}}\rho - 2c_0 e^{\frac{x}{\lambda}}\rho e^{\frac{x}{\lambda}}c_0^\dagger + \rho e^{\frac{2x}{\lambda}}c_0^\dagger c_0\big) \ ,\end{aligned} \tag{4}$$

$$\mathcal{L}_{\rm damp}\rho = -\frac{i\gamma}{2\hbar}[x, \{p, \rho\}] - \frac{\gamma m\omega}{\hbar}(\bar{N} + 1/2)[x, [x, \rho]] \ . \tag{5}$$

The physical meaning of certain of the terms is of particular interest. The term proportional to E is due to the electrostatic force on an occupied (i.e., charged) dot. The exponential dependence of the tunneling terms is clearly visible. The damping of the oscillator cannot be described entirely satisfactorily in the Markovian limit: one cannot simultaneously achieve translational invariance, positivity of the density matrix, and relaxation towards canonical equilibrium. The form given above does not satisfy strict positivity; the quantitative consequences of this shortcoming turned out to be negligible[23]. To proceed further, one considers the electronic diagonal elements $\rho_{00}(t) = \langle 0\,|\rho(t)|0\rangle$ and $\rho_{11}(t) = \langle 1\,|\rho(t)|1\rangle$, where

$|1\rangle = c_0^\dagger|0\rangle$. These objects are still full density matrices in the phonon space and satisfy

$$\dot{\rho}_{00}(t) = \frac{1}{i\hbar}[H_{\rm osc}, \rho_{00}(t)] - \frac{\Gamma_L}{2}(e^{-\frac{2x}{\lambda}}\rho_{00}(t) + \rho_{00}(t)e^{-\frac{2x}{\lambda}}) + \Gamma_R e^{\frac{x}{\lambda}}\rho_{11}(t)e^{\frac{x}{\lambda}} + \mathcal{L}_{\rm damp}\,\rho_{00}(t)\ ,$$
$$\dot{\rho}_{11}(t) = \frac{1}{i\hbar}[H_{\rm osc} - eEx, \rho_{11}(t)] + \Gamma_L e^{-\frac{x}{\lambda}}\rho_{00}(t)e^{-\frac{x}{\lambda}} - \frac{\Gamma_R}{2}(e^{\frac{2x}{\lambda}}\rho_{11}(t) + \rho_{11}(t)e^{\frac{2x}{\lambda}}) + \mathcal{L}_{\rm damp}\,\rho_{11}(t). \tag{6}$$

III. CURENT AND NOISE

A. Analytical development

The current through the system is given by

$$I^{\rm stat} = e\Gamma_L {\rm Tr}_{\rm osc}(e^{-\frac{2x}{\lambda}}\rho_{00}^{\rm stat}) = e\Gamma_R {\rm Tr}_{\rm osc}(e^{\frac{2x}{\lambda}}\rho_{11}^{\rm stat})\ . \tag{7}$$

The trace is carried out over the oscillator basis and $\rho_{nn}^{\rm stat} = \lim_{t\to\infty}\rho_{nn}(t)$. To find the stationary solution, one needs to truncate the oscillator basis at some suitably large value N (in practice, N may reach 100 before convergence is achieved); since the resulting linear system has dimensions $2N^2 \times 2N^2$ (single-dot), or $10N^2 \times 10N^2$ (triple-dot), this becomes a critical issue. The method of solving this vast numerical task is commented on below.

Let us next consider the calculation of noise. In quantum optics one often resorts to a result known as the Quantum Regression Theorem; this allows the calculation of any multi-time correlation function of *system operators*. Unfortunately, in NEMS this theorem can be applied only under very restricted circumstances: it *can* be used to calculate the noise (which is essentially the average of a product of current operators) *within* the three-dot device[25] (because the current operators $\hat{I}_{LC}$ and $\hat{I}_{RC}$ operate within the "system"), while it is unapplicable for the single-dot case (and many other NEMS systems as well) because there the current operators involve operators belonging both to the baths (i.e., the electronic leads) and the system. A more general method is thus called for.

In order to compute the noise spectrum, we follow the ideas of Gurvitz and Prager[34], and introduce number-resolved density-matrices $\rho_{ii}^{(n)}$, where n is the number of electrons

tunnelled into the right lead by time t. Obviously, $\rho_{ii}(t) = \sum_n \rho_{ii}^{(n)}(t)$. The $\rho_{ii}^{(n)}$ obey

$$\begin{aligned}
\dot{\rho}_{00}^{(n)}(t) &= \frac{1}{i\hbar}[H_{\rm osc}, \rho_{00}^{(n)}(t)] + \mathcal{L}_{\rm damp}\,\rho_{00}^{(n)}(t) \\
&\quad - \frac{\Gamma_L}{2}\{e^{-\frac{2x}{\lambda}}, \rho_{00}^{(n)}(t)\} + \Gamma_R e^{\frac{x}{\lambda}}\rho_{11}^{(n-1)}(t)e^{\frac{x}{\lambda}}\ , \\
\dot{\rho}_{11}^{(n)}(t) &= \frac{1}{i\hbar}[H_{\rm osc} - eEx, \rho_{11}^{(n)}(t)] + \mathcal{L}_{\rm damp}\,\rho_{11}^{(n)}(t) \\
&\quad - \frac{\Gamma_R}{2}\{e^{\frac{2x}{\lambda}}, \rho_{11}^{(n)}(t)\} + \Gamma_L e^{-\frac{x}{\lambda}}\rho_{00}^{(n)}(t)e^{-\frac{x}{\lambda}}\ ,
\end{aligned} \tag{8}$$

with $\rho_{11}^{(-1)}(t) \equiv 0$. The mean current and the zero-frequency shot noise spectrum are given by[35]

$$I = e\frac{d}{dt}\sum_n nP_n(t)\Big|_{t\to\infty} = e\sum_n n\dot{P}_n(t)\Big|_{t\to\infty}, \tag{9}$$

$$S(0) = 2e^2\frac{d}{dt}\Big[\sum_n n^2P_n(t) - \Big(\sum_n nP_n(t)\Big)^2\Big]\Big|_{t\to\infty}, \tag{10}$$

where $P_n(t) = {\rm Tr}_{\rm osc}[\rho_{00}^{(n)}(t) + \rho_{11}^{(n)}(t)]$ are the probabilities of finding n electrons in the right lead by time t, i.e. precisely the objects needed for the FCS discussed below. We find $I = \sum_n n\dot{P}_n(t) = \Gamma_R{\rm Tr}_{\rm osc}\big(e^{\frac{2x}{\lambda}}\rho_{11}(t)\big)$, i.e. one recovers the stationary current found above. In a similar fashion, $\sum_n n^2\dot{P}_n(t) = \Gamma_R{\rm Tr}_{\rm osc}\big[e^{\frac{2x}{\lambda}}\big(2\sum_n n\rho_{11}^{(n)}(t) + \rho_{11}(t)\big)\big]$, whose large-time asymptotics determines the shot noise according to (10). We have developed a generating function technique in Ref. 19 to extract this large-time limit. Here we skip the technical details; the upshot is that the zero-frequency noise, and thereby the Fano factor $F \equiv S(0)/2eI$, can be expressed in terms of the pseudoinverse of the Liouvillean (and the static limit of the density matrix known already from the current calculation):

$$F = 1 - \frac{2e\Gamma_R}{I}{\rm Tr}_{\rm osc}\left(e^{\frac{2x}{\lambda}}\left[\mathcal{Q}\mathcal{L}^{-1}\mathcal{Q}\begin{pmatrix}\Gamma_R e^{\frac{x}{\lambda}}\rho_{11}^{\rm stat}e^{\frac{x}{\lambda}} \\ 0\end{pmatrix}\right]_{11}\right)\ . \tag{11}$$

Here $\mathcal{Q}$ is a projection operator that projects away from the stationary state, for which the Liouvillean has the eigenvalue zero. The crucial point is that the pseudoinverse $\mathcal{R}$ of the Liouvillean, defined as $\mathcal{Q}\mathcal{L}^{-1}\mathcal{Q} \equiv \mathcal{R}$ is tractable by similar numerical methods as used in the evaluation of the current. In our discussion of the full counting statistics given below, we analyze a toy-model to illustrate some properties of the pseudoinverse $\mathcal{R}$.

B. Comment on numerics; some results

As mentioned above, the superoperator structure of the Liouville equation leads to large matrices of the order of $N^2 \times N^2$, where N is the number of low-energy states kept in the calculation. A further complication arises from the fact that the stationary limit corresponds to the zero eigenvalue of the Liouvillean, $\mathcal{L}\rho = 0$, forcing one to deal with singular matrices. The problems with the memory size can be circumvented by using iterative methods in which only $\mathcal{L}A$ for a given A is needed ($N \times N$ numbers), and one avoids the storage of the full $\mathcal{L}$ ($N^2 \times N^2$ numbers). Using an iterative method raises the questions of convergence, and the speed of convergence. We found that the so-called Arnoldi iteration technique was sufficient for our purposes (see Appendix A in Ref. 25), provided that one uses a suitable preconditioning. While there exists a substantial empirical body of knowledge of how to carry out the preconditioning, we are not aware of a complete algorithm. As an example, when solving for the pseudoinverse $\mathcal{R}$, we used the inverse of the "Sylvester part" $\mathcal{L}_0$ of $\mathcal{L}$ as preconditioner[26]; finding the inverse of $\mathcal{L}_0$ is a relatively fast procedure. When calculating the noise (which amounts to solving an equation of the type $\mathcal{L}\mathbf{x} = \mathbf{b}$, where the vector $\mathbf{b}$ belongs in the range of $\mathcal{L}$), we used the generalized minimum residual method (GMRes)[36]. Again, appropriate preconditioning was crucial.

Figure 2 shows a set of current vs. damping curves for the single-dot shuttle. We draw attention to the following features. As damping is decreased, the current increases, approaching asymptotically the value $I = 1/2\pi \simeq 0.16$, i.e. one electron is transferred per cycle. In other words, this value of the current indicates that the shuttling transition has taken place, even in the quantum regime. The transition is not as sharp as found in the classical case[4]. For large values of damping the current is much smaller, and scales with the tunneling rate Γ. Very interestingly, we see a sharp increase in the current even without electric field, $E = 0$. Classically this does not happen, and therefore we interpret this cross-over of being due to quantum shot noise.

We have in several occasions promoted the use of Wigner functions as an interpretative tool for the numerical results obtained for the stationary density matrix. The Wigner representation of the GME has also turned out to be a useful starting point for further analytic work[26,29,37]. These phase-space representations have a simple form in the classical limit: the Wigner representation of a regularly moving harmonic oscillator is an ellipse. On

the other hand, irregular motion under the influence of external noise gives rise to a Gaussian probability distribution centered at the origin. The *charge resolved* Wigner functions ($n = 0$ corresponds to an empty dot, while $n = 1$ represents the occupied dot) are defined as

$$W_{nn}(X,P) = \int_{-\infty}^{\infty} \frac{dy}{2\pi\hbar} \left\langle X - \frac{y}{2} \right| \rho_{nn}^{\rm stat} \left| X + \frac{y}{2} \right\rangle \exp\bigl(i\frac{Py}{\hbar}\bigr), \tag{12}$$

and some representative results are given in Fig. 3. As expected, as damping is decreased, the fuzzy central spot evolves into a ring. The finite thickness of the ring is due to thermal noise, the randomness of the charge transport processes, and the position–momentum uncertainty. The earmark of shuttling are the asymmetric, banana-shaped areas observed for weakest damping: here one observes a strong correlation between the occupancy of the dot, and the position and momentum. Thus, there is a large probability to have an occupied dot with a negative position coordinate and positive velocity (the dot has been filled in the neighborhood of the left contact), while there is a large probability of having an empty dot at positive x-values and negative velocity, i.e. on the return journey from the right contact. – As the system approaches the classical limit, the thickness of the Wigner ring shrinks; this is illustrated in Fig. 4. As mentioned above, we expect that the noise of the quantum shuttle yields additional information about the nature of the charge transfer process. Figure 5 shows some of our numerical results. In the top panel we see a relatively sharp cross-over if the tunneling length is larger than the length scale $x_0 = \sqrt{\hbar/(m\omega)}$, i.e. as one aproaches the classical limit. In the bottom panel we show the Fano factor for the same parameters as in the top panel. One should note that a logarithmic scale is used, thus one observes (i) a huge enhancement at the tunneling cross-over, in particular for parameters approaching the semiclassical limit, and (ii) tiny Fano factors below the shuttling cross-over. Thus, even well in the quantum regime shuttling is a highly ordered charge transfer process.

Figure 6 shows the phase-space plot for the parameter values indicated by the asterisk in Fig. 5. The interpretation is very suggestive: for these parameters tunneling and shuttling *co-exist*. Our numerics thus confirm the suggestion put forward in the analytical study of Ref. 29. The large value of the Fano factor can be understood as a slow switching process between the two possible current channels (tunneling and shuttling). In the next section we elaborate this point further.

IV. FULL COUNTING STATISTICS

A. Calculational procedure

We begin by introducing some notation. We recall that the Liouvillean, which is a non-hermitian operator, has a single eigenvalue equal to zero with $\hat{\rho}^{\rm stat}$ being the corresponding (normalized and unique) right eigenvector, we denote this eigenvector by $|0\rangle\!\rangle$. The corresponding left eigenvector is the identity operator $\hat{1}$ which we denote by $\langle\!\langle\tilde{0}|$, and we have $\langle\!\langle\tilde{0}|0\rangle\!\rangle \equiv {\rm Tr}(\hat{1}^\dagger\hat{\rho}^{\rm stat}) = 1$. The pair of eigenvectors allows us to define the complementary projectors $\mathcal{P} \equiv |0\rangle\!\rangle\langle\!\langle\tilde{0}|$ and $\mathcal{Q} \equiv 1 - \mathcal{P}$ obeying the relations $\mathcal{P}\mathcal{L} = \mathcal{L}\mathcal{P} = 0$ and $\mathcal{Q}\mathcal{L}\mathcal{Q} = \mathcal{L}$. We will also need the pseudoinverse of the Liouvillean $\mathcal{R} \equiv \mathcal{Q}\mathcal{L}^{-1}\mathcal{Q}$, which is well-defined, since the inversion is performed only in the subspace spanned by $\mathcal{Q}$, where $\mathcal{L}$ is regular. Rather than attempting to calculate the complete probability distribution $P_n(t) = {\rm Tr}\left[\hat{\rho}^{(\rm n)}(\rm t)\right]$ directly, it turns out to be easier to evaluate the cumulant generating function $S(t,\chi)$,

$$e^{S(t,\chi)} = \sum_{n=-\infty}^{\infty} P_n(t)e^{in\chi}. \tag{13}$$

From $S(t,\chi)$ we find the m'th cumulant of the charge distribution by taking the m-th derivative with respect to the counting field χ at $\chi = 0$:

$$\langle\!\langle n^m\rangle\!\rangle(t) = \frac{\partial^m S}{\partial(i\chi)^m}|_{\chi=0}, \tag{14}$$

and from the knowledge of all cumulants we can reconstruct $P_n(t)$. The cumulants of the current in the stationary limit $t \to \infty$ are given by the time derivative of the charge cumulants:

$$\langle\!\langle I^m\rangle\!\rangle = \frac{d}{dt}\langle\!\langle n^m\rangle\!\rangle(t)\big|_{t\to\infty}. \tag{15}$$

The first two current cumulants give the average current running through the system and the zero-frequency current noise, respectively. We have recently developed a systematic perturbation theory to calculate the higher cumulants[22], and we just quote the final results:

$$\begin{aligned}
\langle\!\langle I\rangle\!\rangle &= \langle\!\langle\tilde{0}|\mathcal{I}\,|0\rangle\!\rangle,\\
\langle\!\langle I^2\rangle\!\rangle &= \langle\!\langle\tilde{0}|\mathcal{J}|0\rangle\!\rangle - 2\langle\!\langle\tilde{0}|\mathcal{I}\mathcal{R}\mathcal{I}\,|0\rangle\!\rangle,\\
\langle\!\langle I^3\rangle\!\rangle &= \langle\!\langle\tilde{0}|\mathcal{I}\,|0\rangle\!\rangle - 3\langle\!\langle\tilde{0}|\mathcal{I}\mathcal{R}\mathcal{J} + \mathcal{J}\mathcal{R}\mathcal{I}\,|0\rangle\!\rangle - 6\langle\!\langle\tilde{0}|\mathcal{I}\mathcal{R}(\mathcal{R}\mathcal{I}\mathcal{P} - \mathcal{I}\mathcal{R})\mathcal{I}\,|0\rangle\!\rangle,
\end{aligned} \tag{16}$$

where

$$\mathcal{I} = \mathcal{I}^+ - \mathcal{I}^- \tag{17}$$

$$\mathcal{J} = \mathcal{I}^+ + \mathcal{I}^-. \tag{18}$$

The explicit expressions for the current superoperators $\mathcal{I}^{\pm}$ depend on the problem at hand; two examples are given in Ref. 22 (see also the analytic toy model discussed below). We emphasize the utility of these formulae: they imply that once the hard numerical problems with the stationary case are solved, the higher cumulants are essentially immediately accessible. Using the systematic perturbation theory developed in Ref. 22 algebraic formulas for the fourth, fifth etc. cumulant can be generated with computer routines performing symbolic manipulations. In Fig. 7 we show numerical results for the first three cumlants for the single-dot shuttle.

B. Toy model

The general formulation for calculation of higher cumulants given above is very practical also in analytic calculations. Here we illustrate it by considering a toy model, for which the current and noise are very well-known, while the third cumulant cannot be considered as a standard result. Specifically, we consider a two level system, whose occupation probabilities obey the Master equation ($\mathbf{p} = (p_0 \quad p_1)^{\mathrm{T}}$)

$$\dot{\mathbf{p}} = \mathcal{L}\mathbf{p} = \begin{pmatrix} -\Gamma_L & \Gamma_R \\ \Gamma_L & -\Gamma_R. \end{pmatrix} \mathbf{p} \tag{19}$$

The relevance of this model to the shuttling dynamics is based on the fact that in the coexistence regime there are two "states": the incoherent tunneling current channel (reflected by the central spot in the Wigner function description), and the orderly shuttling channel (reflected) by the ring, and that the system can be visualized as fluctuating between these two states. The bare two-level system, as discussed in this section, needs a slight modification to take into account that in the coexistence regime one deals with *current channels* and not states, and further discussion can be found in Ref. 22, see also Ref. 38 for a related model. The Liouvillean of Eq. (19) has the following right and left null vectors:

$$|0\rangle\rangle = \frac{1}{\Gamma_L + \Gamma_R} \begin{pmatrix} \Gamma_R \\ \Gamma_L \end{pmatrix}, \quad \langle\langle\tilde{0}| = \begin{pmatrix} 1 & 1 \end{pmatrix}, \tag{20}$$

which satisfy $\mathcal{L}|0\rangle\!\rangle = 0 = \langle\!\langle\tilde{0}|\mathcal{L}$ and $\langle\!\langle\tilde{0}|0\rangle\!\rangle = 1$, as is readily verified. We can immediately form the projectors $\mathcal{P}$ and $\mathcal{Q}$:

$$\mathcal{P} = |0\rangle\!\rangle\langle\!\langle\tilde{0}| = \frac{1}{\Gamma_R + \Gamma_L}\begin{pmatrix}\Gamma_R & \Gamma_R\\ \Gamma_L & \Gamma_R\end{pmatrix}, \quad \mathcal{Q} = 1 - \mathcal{P} = \frac{1}{\Gamma_R + \Gamma_L}\begin{pmatrix}\Gamma_L & -\Gamma_R\\ -\Gamma_L & \Gamma_R\end{pmatrix}. \tag{21}$$

We also record the current superoperator:

$$\mathcal{I}_{0R} = \begin{pmatrix}0 & \Gamma_R\\ 0 & 0\end{pmatrix}. \tag{22}$$

Next, we need the eigenvector $|\nu\rangle\!\rangle$ of $\mathcal{L}$ which does not belong to the null space (here, the situation is quite simple because the full problem is 2-dimensional with a 1-dimensional null space), and the associated eigenvalue λ_ν. We readily find

$$\lambda_\nu = -(\Gamma_R + \Gamma_L); \quad |\nu\rangle\!\rangle = \begin{pmatrix}1\\ 1\end{pmatrix}; \quad \langle\!\langle\tilde{\nu}| = \frac{1}{\Gamma_R + \Gamma_L}\begin{pmatrix}\Gamma_L & \Gamma_R\end{pmatrix}, \tag{23}$$

and can thus compute the pseudoinverse $\mathcal{R}$:

$$\mathcal{R} = \mathcal{Q}\mathcal{L}^{-1}\mathcal{Q} = \frac{1}{\lambda_\nu}|\nu\rangle\!\rangle\langle\!\langle\tilde{\nu}| = -\frac{1}{(\Gamma_R + \Gamma_L)^2}\begin{pmatrix}\Gamma_L & -\Gamma_R\\ -\Gamma_L & \Gamma_R\end{pmatrix} = \frac{1}{\lambda_\nu}\mathcal{Q}. \tag{24}$$

With these results at hand, the evaluation of various cumulants is reduced to simple matrix multiplications, and we quote the results

$$\langle\!\langle\mathcal{I}\rangle\!\rangle = \frac{\Gamma_L\Gamma_R}{\Gamma_L + \Gamma_R} \tag{25}$$

$$\langle\!\langle\mathcal{I}^2\rangle\!\rangle = \frac{\Gamma_R^2 + \Gamma_L^2}{(\Gamma_R + \Gamma_L)^2}\langle\!\langle\mathcal{I}\rangle\!\rangle \tag{26}$$

$$\langle\!\langle\mathcal{I}^3\rangle\!\rangle = \frac{\Gamma_R^4 - 2\Gamma_R^3\Gamma_L + 6\Gamma_R^2\Gamma_L^2 - 2\Gamma_R\Gamma_L^3 + \Gamma_L^4}{(\Gamma_R + \Gamma_L)^2}\langle\!\langle\mathcal{I}\rangle\!\rangle. \tag{27}$$

The first two results are well-known from the literature (see, e.g., Ref. 12), however the third cumulant may be new. We believe that the above method of calculation can be very useful in extending several previous results, such as those obtained in by Kießlich et al.[39].

C. Experimental status

To summarize the experimental status very shortly, we do not believe that the shuttling transition has been observed so far. Having stated this negative conclusion, we hasten to

point out that we think that the experimental situation is very promising, and that a crucial experiment could be just behind the corner.

Two key experiments have been reported, which contain several important ingredients. In the experiment of Park *et al.*[5] a C_{60} molecule was placed in a break junction, and the current-voltage characteristics showed clear indications of effects due to vibrational quanta. We believe that the observed values of the current are too small to be attributed to shuttling (recall that the shuttling current has the universal value of $1/2\pi$), and that the system is in the tunneling limit. In the experiment of Erbe *et al.*[40] the system was driven: indeed electrons were shuttled, but the experiment was not designed to observe the shuttling transition as a function of a control parameter. Our optimism is based on a number of new structures that are currently being explored in the literature, and in particular we find the structures of Scheible *et al.*[41], where a soft silicon pillar forms the movable part, very promising. We also believe that the theoretical methods outlined above are suitable for modeling quantitatively the forthcoming experiments.

V. CONCLUSION

We have discussed at length some properties of a nanomechanical device, the quantum shuttle, which we believe can be an important component in future applications, for example measurements of very small displacements. While the quantitative results of the present work apply to very specific, and strongly idealized models, we believe that many of the phenomena we address are generic, and will be observed in near future. One of the central messages we want to pass is that the fluctuation properties of these devices contain a wealth of information, and that this information may be essential in identifying the key charge transfer processes in these devices.

---

* Electronic address: antti@mic.dtu.dk

† Electronic address: cf@mic.dtu.dk

‡ Electronic address: tno@mic.dtu.dk

§ Electronic address: ad@mic.dtu.dk

[1] H. G. Craighead, Science **290**, 1532 (2000).

[2] A. N. Cleland, *Foundations of Nanomechanics*, Advanced Texts in Physics (Springer, Berlin, 2003).

[3] M. Blencowe, Physics Reports **395**, 159 (2004).

[4] L. Y. Gorelik, A. Isacsson, M. V. Voinova, B. Kasemo, R. I. Shekhter, and M. Jonson, Phys. Rev. Lett. **80**, 4526 (1998), cond-mat/9711196.

[5] H. Park, J. Park, A. K. L. Lim, E. H. Anderson, A. P. Alivisatos, and P. L. McEuen, Nature **407**, 57 (2000).

[6] D. Boese and H. Schoeller, Europhys. Lett. **54**, 668 (2001), cond-mat/0012140.

[7] K. D. McCarthy, N. Prokof'ev, and M. T. Tuominen, Phys. Rev. B **67**, 245415 (2003), cond-mat/0205419.

[8] K. Flensberg, Phys. Rev. B **68**, 205323 (2003), cond-mat/0302193.

[9] S. Braig and K. Flensberg, Phys. Rev. B **68**, 205324 (2003), cond-mat/0303236.

[10] D. Fedorets, L. Y. Gorelik, R. I. Shekhter, and M. Jonson, Europhys. Lett. **58**, 99 (2002), cond-mat/0104200.

[11] S. Kogan, *Electronic Noise and Fluctuations in Solids* (Cambridge University Press, Cambridge, 1996).

[12] Y. M. Blanter and M. Büttiker, Physics Reports **336**, 1 (2000).

[13] C. Beenakker and C. Schönenberger, Physics Today **56**, 37 (2003).

[14] A. Mitra, I. Aleiner, and A. J. Millis, *Phonon effects in molecular transistors: Quantum and classical treatment* (2003), cond-mat/0311503.

[15] F. Pistolesi, Phys. Rev. B **69**, 245409 (2004), cond-mat/0401361.

[16] A. D. Armour, *Current noise of a single-electron transistor coupled to a nano-mechanical resonator* (2004), cond-mat/0401387.

[17] N. M. Chtchelkatchev, W. Belzig, and C. Bruder, *Charge transport through a set with a mechanically oscillating island* (2004), cond-mat/0401486.

[18] A. Isacsson and T. Nord, Europhys. Lett. **66**, 708 (2004), cond-mat/0402228.

[19] T. Novotný, A. Donarini, C. Flindt, and A.-P. Jauho, Phys. Rev. Lett. **92**, 248302 (2004), cond-mat/0402597.

[20] Y. M. Blanter, O. Usmani, and Y. V. Nazarov, Phys. Rev. Lett. **93**, 136802 (2004), cond-mat/0404615.

[21] B. Reulet, J. Senzier, and D. E. Prober, Phys. Rev. Lett. **91**, 196601 (2004).

[22] C. Flindt, T. Novotný, and A.-P. Jauho, *Full counting statistics of nano-electromechanical systems* (2004), cond-mat/0410322.

[23] T. Novotný, A. Donarini, and A.-P. Jauho, Phys. Rev. Lett. **90**, 256801 (2003), cond-mat/0301441.

[24] A. Donarini, T. Novotný, and A.-P. Jauho, Semicond. Sci. Technol. **19**, S430 (2004), cond-mat/0401357.

[25] C. Flindt, T. Novotný, and A.-P. Jauho, Phys. Rev. B (2004), cond-mat/0405512.

[26] A. Donarini, Ph.D. thesis, MIC, Technical University of Denmark (2004), URL `http://www.mic.dtu.dk/research/TheoreticalNano/publications/Theses.htm`.

[27] R. I. Shekhter, Y. Galperin, L. Y. Gorelik, A. Isacsson, and M. Jonson, J. Phys. Condens. Matter **15**, R441 (2003).

[28] D. Fedorets, Phys. Rev. B **68**, 033106 (2003).

[29] D. Fedorets, L. Y. Gorelik, R. I. Shekhter, and M. Jonson, Phys. Rev. Lett. **92**, 166801 (2004), cond-mat/0311105.

[30] A. Y. Smirnov, L. G. Mourokh, and N. J. M. Horing, Phys. Rev. B **69**, 155310 (2004), cond-mat/0311052.

[31] A. D. Armour and A. MacKinnon, Phys. Rev. B **66**, 035333 (2002), cond-mat/0204521.

[32] C. W. Gardiner and P. Zoller, *Quantum Noise* (Springer, 2000), 2nd ed.

[33] U. Weiss, *Quantum Dissipative Systems*, vol. 10 of *Series in Modern Condensed Matter Physics* (World Scientific, 1999), 2nd ed.

[34] S. A. Gurvitz and Y. S. Prager, Phys. Rev. B **53**, 15932 (1996).

[35] B. Elattari and S. A. Gurvitz, Physics Letters A **292**, 289 (2002).

[36] C. Flindt, Master's thesis, MIC, Technical University of Denmark (2004), URL `http://www.mic.dtu.dk/research/TheoreticalNano/publications/Theses.htm`.

[37] D. Fedorets, L. Y. Gorelik, R. I. Shekhter, and M. Jonson, *Spintronics of a nanoelectromechanical shuttle* (2004), cond-mat/0408591.

[38] A. N. Jordan and E. V. Sukhorukov, *Transport statistics of bistable systems* (2004), cond-mat/0406261.

[39] G. Kießlich, A. Wacker, and E. Schöll, Phys. Rev. B **68**, 125320 (2003), cond-mat/0303025.

[40] A. Erbe, C. Weiss, W. Zwerger, and R. H. Blick, Phys. Rev. Lett. **87**, 096106 (2001), cond-mat/0011429.

[41] D. C. Scheible and R. H. Blick, Appl. Phys. Lett. **84**, 4632 (2004).

Figures

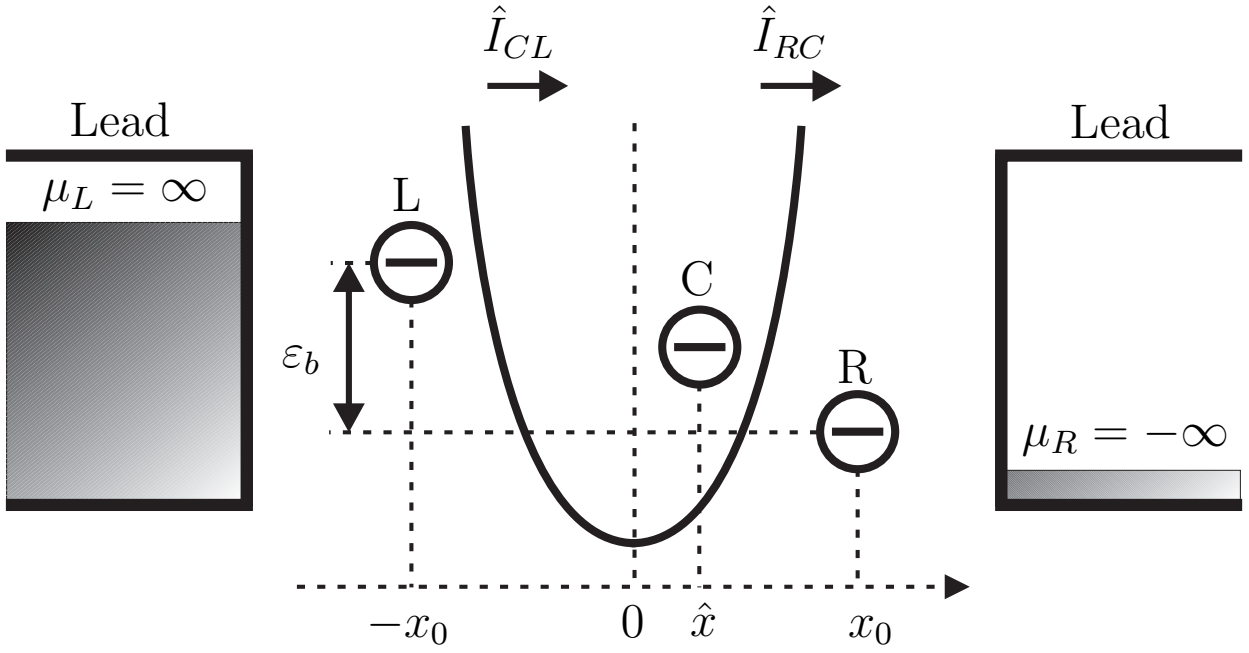

FIG. 1: Schematic picture of a three-dot system, introduced by Armour and MacKinnon[31]. The outer dots are fixed — the left one (L) at the position $-x_0$ and the right one (R) at x_0, while the central one (C) can move (position $\hat{x}$) in a harmonic confining potential. It also interacts with a heat bath causing damping and thermal noise. The outer dots whose respective energy levels are de-aligned by the device bias (ε_b) are coupled to the full or empty electronic reservoirs (leads), respectively. The current flows within the system due to tunneling between the left and central dot and the central and right dot. (Reproduced from Ref. 23).

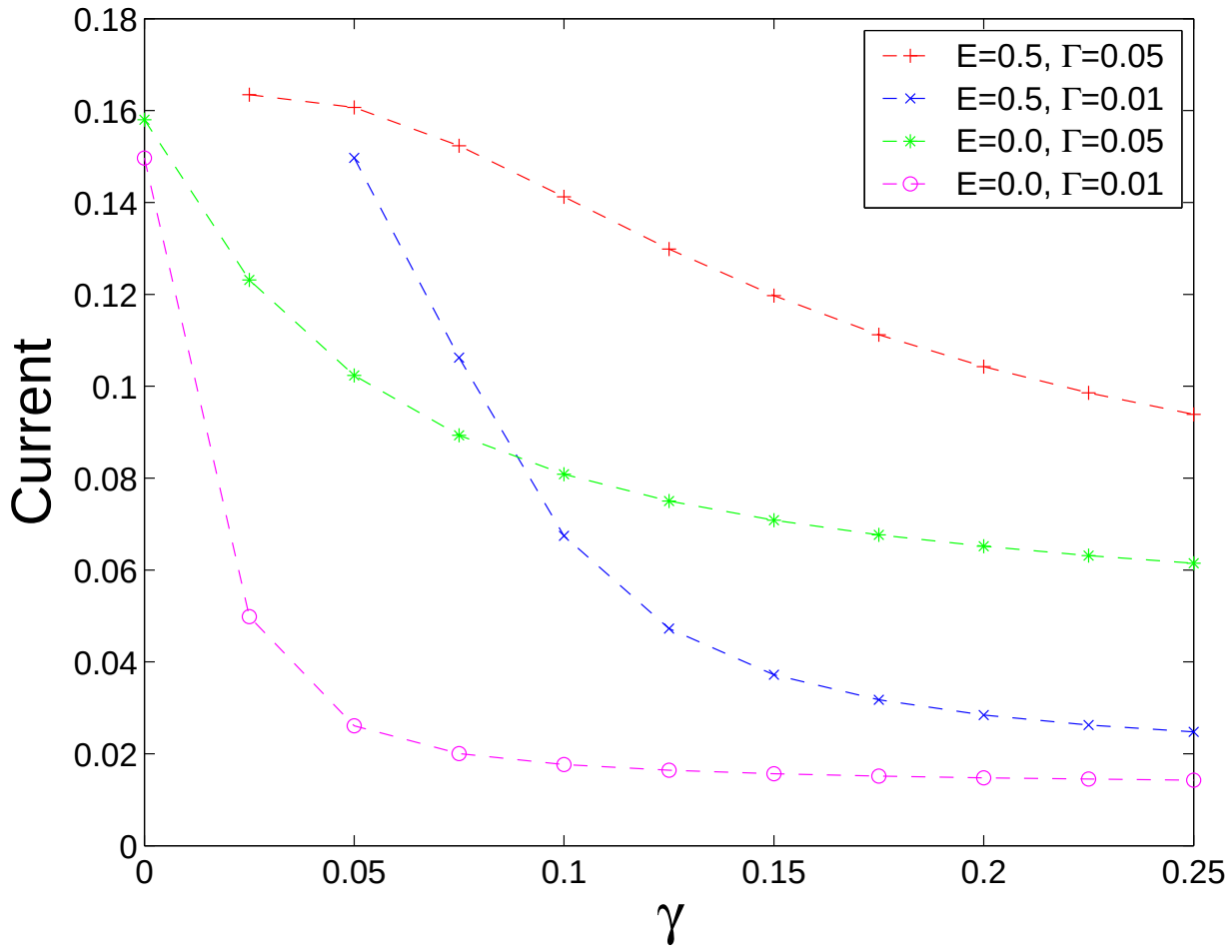

FIG. 2: $I-\gamma$ curve. The damping dependence of the stationary current through the single-dot shuttle for different transfer rates and electric fields. Their values are $d = 0.5x_0, \Gamma = 0.05\hbar\omega$ (pluses; corresponds to Fig. 3), $d = 0.5x_0, \Gamma = 0.01\hbar\omega$ (circles), $d = 0.0, \Gamma = 0.05\hbar\omega$ (asterisks), $d = 0.0, \Gamma = 0.01\hbar$ (crosses). Other parameters are $\lambda = x_0, T = 0$. The current is in units of $e\omega$ while γ in $\hbar\omega$. (Reproduced from Ref.23)

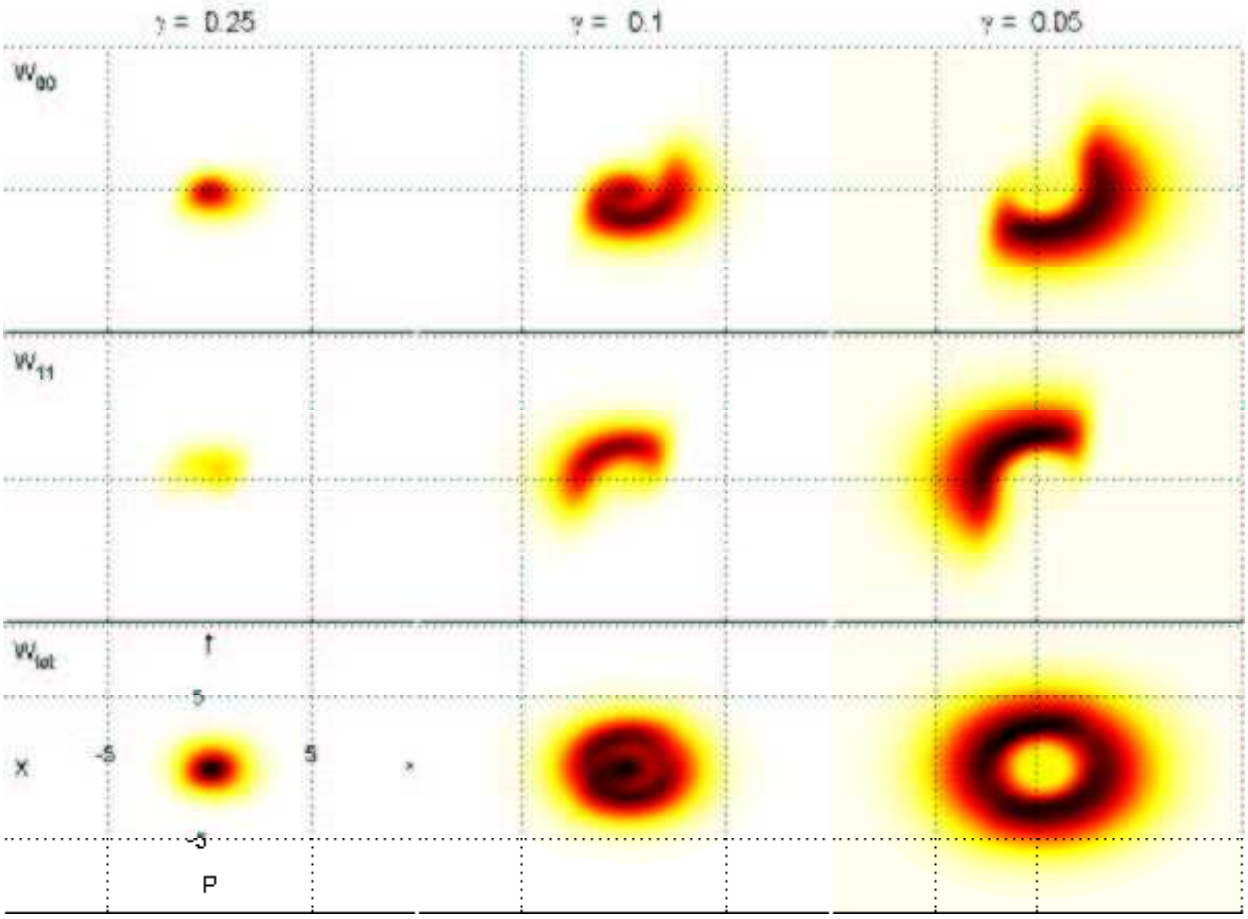

FIG. 3: Phase space picture of the tunnelling-to-shuttling crossover. The respective rows show the Wigner distribution functions for the discharged (W_{00}), charged (W_{11}), and both ($W_{\rm tot}$) states of the oscillator in the phase space (horizontal axis – coordinate in units of $x_0 = \sqrt{\hbar/m\omega}$, vertical axis – momentum in $\hbar/x_0$). The values of the parameters are: $\lambda = x_0, T = 0, d = 0.5x_0, \Gamma = 0.05\hbar\omega$. The values of γ are in units of $\hbar\omega$. The Wigner functions are normalized within each column. (Reproduced from Ref. 23)

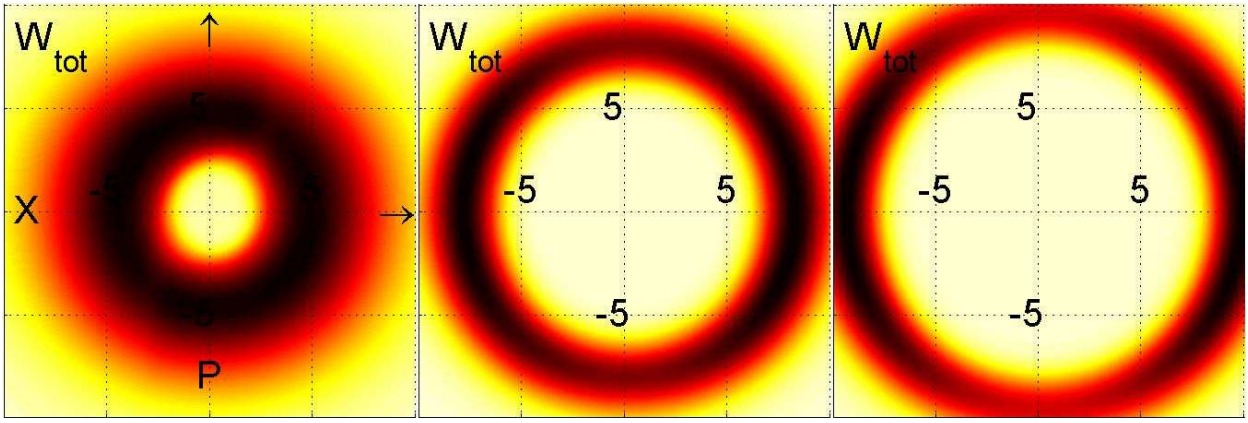

FIG. 4: Transition from quantum limit to classical limit. The "quantum thickness" of the Wigner ring shrinks, and the radius increases, indicating larger maximal velocity, and oscillation amplitude.

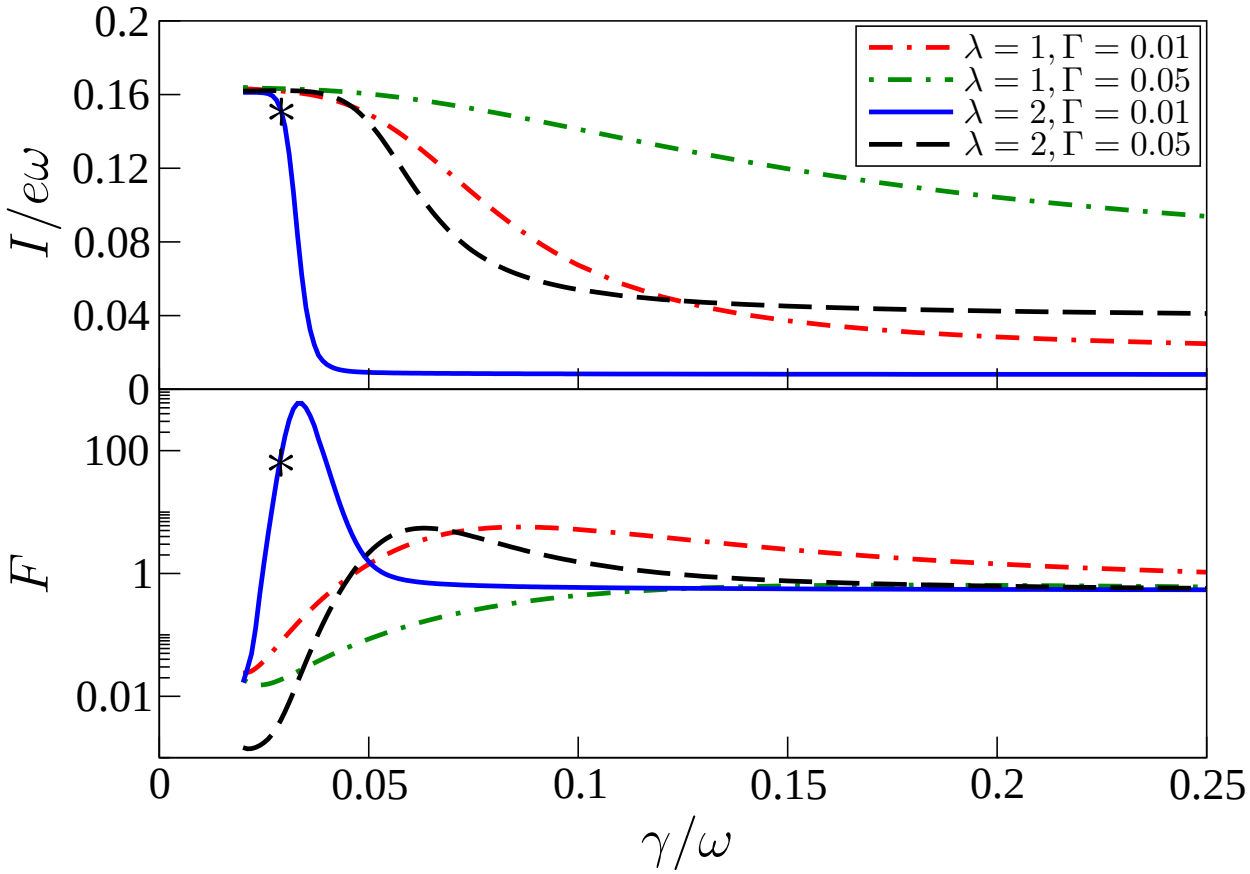

FIG. 5: Current I and Fano factor F vs. damping γ. The γ-dependence of I (upper panel) and F on log scale (lower panel) for different transfer rates Γ and tunnelling lengths λ. The parameters are $\lambda = x_0, \Gamma = 0.01\omega$ (full); $\lambda = x_0, \Gamma = 0.05\omega$ (long dashes); $\lambda = 2x_0, \Gamma = 0.01\omega$ (short dashes); $\lambda = 2x_0, \Gamma = 0.05\omega$ (dots) with $x_0 = \sqrt{\hbar/m\omega}$. Other parameters are $eE/m\omega^2 = 0.5x_0$, $T = 0$. The current is in units of $e\omega$ while γ in units of ω. The asterisk defines the parameters of Wigner distributions in Fig. 6. (Reproduced from Ref. 19.)

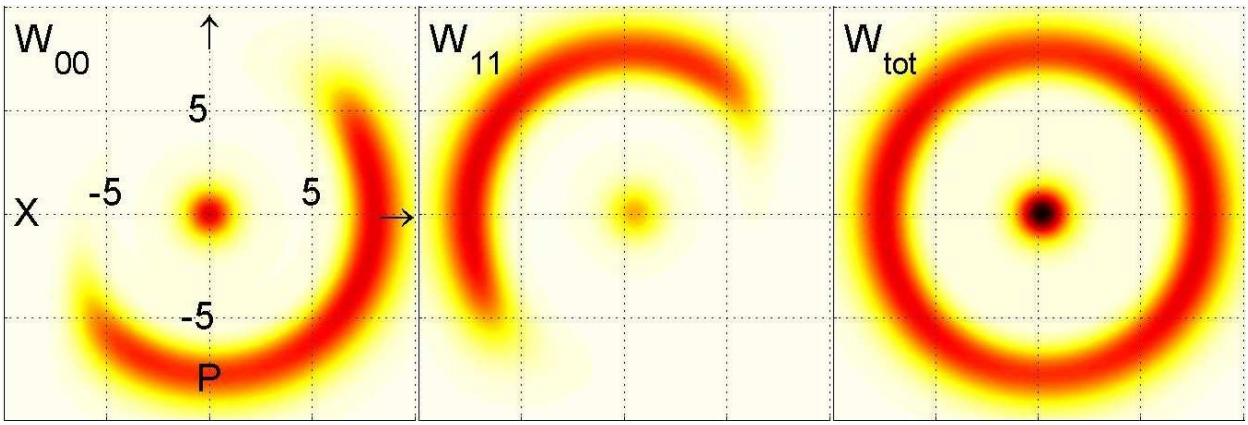

FIG. 6: Phase space picture of the shuttle around the transition where the shuttling and tunnelling regimes coexist. The respective rows show the Wigner distribution functions for the discharged (W_{00}), charged (W_{11}), and both ($W_{\rm tot} = W_{00} + W_{11}$) states of the oscillator in the phase space (horizontal axis – coordinate in units of $x_0 = \sqrt{\hbar/m\omega}$, vertical axis – momentum in $\hbar/x_0$). The values of the parameters are: $\lambda = 2x_0, eE/m\omega^2 = 0.5x_0, \gamma = 0.029\omega, \Gamma = 0.01\omega, T = 0$.

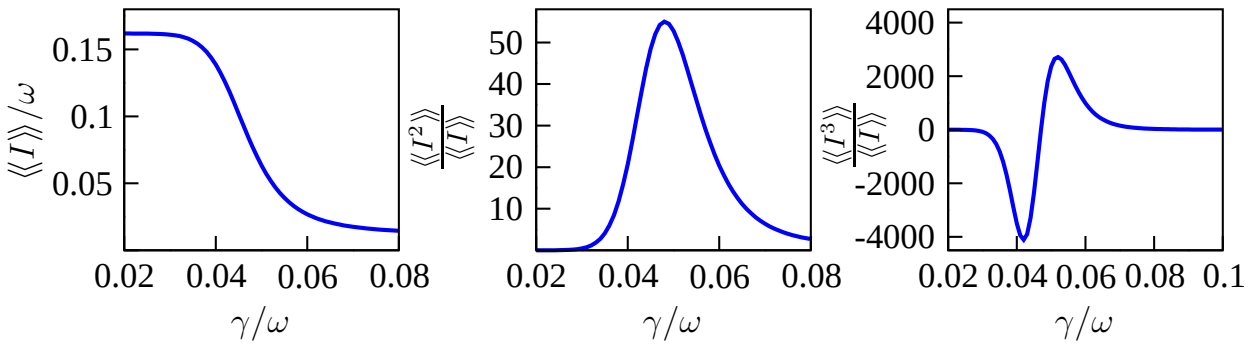

FIG. 7: The first three cumulants for the one-dot shuttle as a function of the damping γ. The parameters are $\lambda = 1.5x_0$, $d = eE/m\omega^2 = 0.5x_0$.